

RSC Advances



This is an *Accepted Manuscript*, which has been through the Royal Society of Chemistry peer review process and has been accepted for publication.

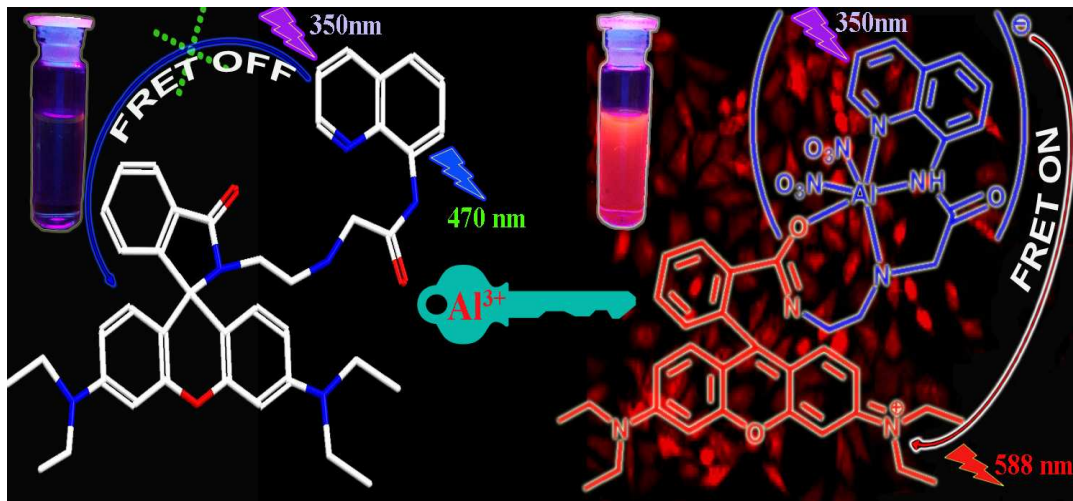
Accepted Manuscripts are published online shortly after acceptance, before technical editing, formatting and proof reading. Using this free service, authors can make their results available to the community, in citable form, before we publish the edited article. This *Accepted Manuscript* will be replaced by the edited, formatted and paginated article as soon as this is available.

You can find more information about *Accepted Manuscripts* in the [Information for Authors](#).

Please note that technical editing may introduce minor changes to the text and/or graphics, which may alter content. The journal's standard [Terms & Conditions](#) and the [Ethical guidelines](#) still apply. In no event shall the Royal Society of Chemistry be held responsible for any errors or omissions in this *Accepted Manuscript* or any consequences arising from the use of any information it contains.

Graphical Abstract

A newly designed FRET-based ratiometric chemosensor (L^1) highly selective for Al^{3+} ions of very low level (up to 6.19×10^{-9} M) has been developed in HEPES buffer (1 mM, pH 7.4; 2% EtOH) at 25 °C. The probe (L^1) could be employed for imaging Al^{3+} ions in living cells.



Cite this: DOI: 10.1039/c0xx00000x

www.rsc.org/xxxxxx

ARTICLE TYPE

A FRET based 'off-on' molecular switch: an effective design strategy for selective detection of nanomolar Al³⁺ ions in aqueous media[†]Buddhadeb Sen,^a Siddhartha Pal,^a Somenath Lohar,^a Manjira Mukherjee,^a Sushil Kumar Mandal,^b Anisur Rahman Khuda-Bukhsh,^b and Pabitra Chattopadhyay*^a⁵ Received (in XXX, XXX) Xth XXXXXXXXX 20XX, Accepted Xth XXXXXXXXX 20XX

DOI: 10.1039/b000000x

A new water soluble rhodamine based Al³⁺ ions selective probe, L¹ was synthesised and characterized by physico-chemico and spectroscopic tools. In presence of large excess of other competing ions, L¹ specifically binds Al³⁺ ions with concurrent visually observable changes from colourless to pink in electronic spectral behaviour to make possible significant naked eye detection of Al³⁺ ions. On addition of Al³⁺ ions to the solution of L¹ in HEPES buffer (1 mM, pH 7.4; 2% EtOH) at 25 °C, the weak fluorescence intensity at λ_{em} = 470 nm decreases and a new peak (at λ_{em} = 588 nm) increases gradually through fluorescence resonance energy transfer (FRET) process. This ratiometric enhancement helps to detect Al³⁺ ions of very low concentration of 33 nM. The detection limit of L¹ for Al³⁺ ions was estimated to be 6.19 × 10⁻⁹ M using the 3σ method. This probe is also useful for imaging Al³⁺ ions in HeLa cells.

Introduction

Chemosensors for selective detection of various biologically and environmentally relevant metal ions have recently attracted great attention because of their potential use in medicinal and environmental research. Aluminum is the third abundant element in the earth inferior to oxygen and silicon, and people are widely exposed to aluminum due to its widespread use in food additives, aluminum-based pharmaceuticals, and cooking utensils.^{1,2} After absorption, aluminum will become distributed to all tissues in humans and animals, and accumulates in the bone. Some iron binding protein (e.g. transferrin C1 and C2 and ferritin etc.) are the main carrier of Al³⁺ ions in plasma and Al³⁺ ions can enter into the brain and reach the placenta and fetus. Al³⁺ ions may persist for a very long time in various organs and tissues before it is excreted in the urine. Aluminum salts are neurotoxic and are suspected to induce Parkinson's disease³ and senile dementia, commonly known as Alzheimer's disease,⁴ microcytic anemia, dialysis dementia, osteomalacia and even to risk the cancer of lung and bladder.⁵⁻⁸ Thus, aluminum should be regarded as a toxic metal and its concentration in environment ought to be monitored. In 1989, World Health Organization (WHO) listed Al to be one of the food pollution sources and limited aluminum concentration to 200 mg L⁻¹ (7.41 mM) in drinking water. The FAO/ WHO Joint Expert Committee on Food Additives recommended a maximum daily intake of aluminum of 3-10 mg per day/kg-body mass. Furthermore, it is believed that almost 40 % of the world's acid soils are polluted by the effects of aluminum toxicity, which is the key factor for hampering plant (i.e., crop) performance on the acid soils.^{9,10} Based on the above reasons, detection of Al³⁺ ions is crucial in controlling its concentration levels in the environmental monitoring and its

direct impact on human health.

To date, several conventional methods with moderate sensitivity for Al³⁺ ions detection based on atomic absorption spectroscopy (AAS), chromatographic and spectro-photometric techniques have been developed.¹¹ Among these, AAS required expensive instruments and complicated sample preparation processes. Although the other techniques have been developed for detecting the trace amount of Al³⁺ ions, most of them involve the use of harmful chemicals and moreover, the analysis procedures are easily interfered by the variation in pH value of solution and the coexistence of interferential ions. But the spectrofluorimetric method has received considerable attention in recent years due to its simplicity, high sensitivity and real-time monitoring with a low response time.¹²⁻¹⁴

There are several fluorescent sensors for Al³⁺ ions having good selectivity, but this approach has several disadvantages including complicated synthetic procedures, poor water solubility, insensible to biological system and is often interfered by other ions and pH conditions.¹⁵ Sensitive bioimaging of Al³⁺ ions in the cell is a prerequisite for understanding the underlying mechanism about how aluminum ions cause aluminum-induced human diseases. The number of reports of chemosensors that can detect Al³⁺ ions in aqueous media is few and most of them are chelation-enhanced fluorescence (CHEF) / photoinduced electron transfer (PET) based.¹⁵ But there are very few depending on FRET mechanism.¹⁶ The sensors with fluorescence enhancement (turn-on response) through Fluorescence Resonance Energy Transfer (FRET) are of considerable interest as FRET is a distance dependent radiationless transfer of energy from an excited donor fluorophore to a suitable acceptor fluorophore to investigate molecular level interactions.¹⁷ Thus, the development of new ratiometric FRET based sensors for Al³⁺ ions with

improved detection limits in the presence of water is desirable.

Herein we report a newly designed ratiometric FRET based fluorescent sensor (L^1) highly selective for Al^{3+} ions in HEPES buffer (1 mM, pH 7.4; 2% EtOH) at 25 °C. On excitation at 350 nm, the probe, L^1 exhibits a fluorescence maximum at 470 nm which decreases along with the gradual increase of a new peak at 588 nm due to the addition of Al^{3+} ions. This phenomenon is due to the ring-opening of the spirolactam system of rhodamine giving rise to a strong fluorescence emission and also a visual color change of the solution from colorless to pink. Ratiometric responses are more attractive because the ratio between the two emission intensities can be used to measure the analyte concentration and sensor molecule concentration, provide a built-in correction for environmental effects and stability under illumination.^{14,18} Interestingly, the presence of an excess of the other metal ions, viz. alkali (Na^+ , K^+), alkaline earth (Mg^{2+} , Ca^{2+}), and transition metal ions (Cr^{3+} , Mn^{2+} , Fe^{3+} , Co^{2+} , Ni^{2+} , Cu^{2+} , Zn^{2+} , Cd^{2+} , Hg^{2+}) and Pb^{2+} ions does not affect the “switch ON” behavior of the receptor L^1 observed in presence of Al^{3+} ions. Fluorescence microscopic studies confirmed that L^1 could also be used as an imaging probe for the detection of uptake of Al^{3+} ions in HeLa cells.

Experimental section

Materials and methods

High-purity HEPES, 8-aminoquinoline, 2-chloroacetyl chloride and aluminium nitrate nonahydrate were purchased from Sigma Aldrich (India) and rhodamine B, ethylene diamine (en) from E. Merck. Solvents used were spectroscopic grade. All metal salts were used as either their nitrate or their chloride salts. Other chemicals were of analytical reagent grade and used without further purification except when specified. Milli-Q, 18.2 MΩ cm⁻¹ water was used throughout all experiments. A Shimadzu (model UV-1800) spectrophotometer was used for recording electronic spectra. FTIR spectra were recorded using Perkin Elmer FTIR model RX1 spectrometer preparing KBr disk. ¹HNMR spectra were obtained on a Bruker Avance DPX 500 MHz spectrometer and Geol 400 MHz spectrometer, using CDCl₃ solution. Electrospray ionization (ESI) mass spectra were recorded on a Qtof Micro YA263 mass spectrometer. A Systronics digital pH meter (model 335) was used to measure the pH of the solution and the adjustment of pH were done using either 50 mM HCl or NaOH solution. Steady-state fluorescence emission and excitation spectra were recorded with a Hitachi 4500 spectrofluorimeter. Time-resolved fluorescence lifetime measurements were performed using a HORIBA JOBIN Yvon picosecond pulsed diode laser-based time-correlated single-photon counting (TCSPC) spectrometer from IBH (UK) at λ_{ex} = 377 nm and MCP-PMT as a detector. Emission from the sample was collected at a right angle to the direction of the excitation beam maintaining magic angle polarization (54.71). The full width at half-maximum (FWHM) of the instrument response function was 250 ps, and the resolution was 28.6 ps per channel. Data were fitted to multiexponential functions after deconvolution of the instrument response function by an iterative reconvolution technique using IBH DAS 6.2 data analysis software in which reduced χ^2 and weighted residuals serve as

parameters for goodness of fit.

Synthesis of the probe (L^1)

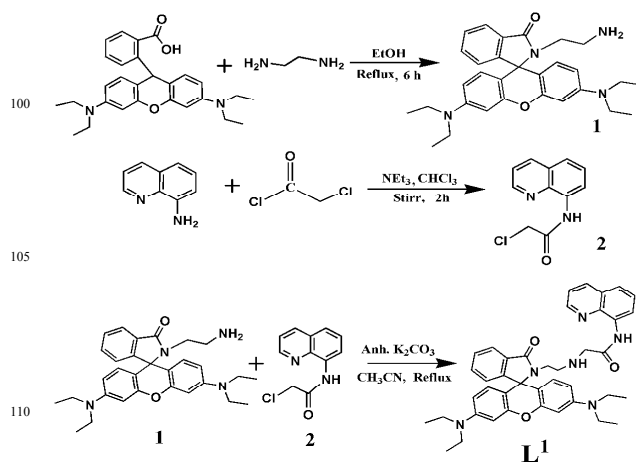
The probe L^1 was synthesised by a 3 step reactions (Scheme 1).

At first, the rhodamine B-en carboxamide (**1**) was prepared following a literature method.¹⁹ Ethylene diamine (en, 4 mL) was added to a solution of rhodamine B (1 g, 2.09 mmol) in ethanol (40 mL). The solution was refluxed for 6 h. Then, the reaction mixture was evaporated under reduced pressure to give orange oil, which was then recrystallized from methanol-water to afford rhodamine B-en carboxamide (**1**) as a light-orange crystal (77%).

Then 2-chloro-N-(quinol-8-yl)acetamide (**2**) was prepared from the reaction of 2-chloroacetyl chloride and 8-aminoquinoline. 2-Chloroacetyl chloride (5.31 mL) was dissolved in chloroform (5 mL) and then added dropwise to a cooled stirred solution of 8-aminoquinoline (2.88 g, 20 mmol) and Et₃N (3.0 mL) in chloroform (10 mL) within 1 h. After being stirred for 2 h at room temperature, the mixture was removed under reduced pressure to obtain a white solid, which was filtered out and extracted with dichloromethane to afford compound **2**.²⁰ Yield: 82 %. mp (°C): 133 ± 2.

In the final step, rhodamine B-en carboxamide (**1**) was taken in dry acetonitrile having anhydrous K₂CO₃ and 2-chloro-N-(quinolin-8-yl)acetamide (**2**) in dry acetonitrile was added dropwise at stirring condition. The resulting reaction mixture was refluxed for 6 h. The volume of the solution was reduced to obtain a solid and then extracted with dichloromethane and finally purified by silica gel column chromatography using dichloromethane as the eluent. Yield: 73 %, mp (°C): 103 ± 2.

C₄₁H₄₄N₆O₃: Anal. Found: C, 73.39; H, 6.46; N, 12.83; Calc.: C, 73.63; H, 6.63; N, 12.57. IR (cm⁻¹): ν_{NH} , 3441; $\nu_{C=C}$, 2970; $\nu_{C=O}$, 1681; $\nu_{C=N}$, 1618; ¹HNMR (400 MHz, CDCl₃): 10.91 (s, 1-NH-CO), 8.43 (dd, 1H), 8.21 (dd, 1H), 8.12 (dd, 1H), 7.45 (m, 2H), 7.08 (dd, 2H), 7.07 (m, 1H), 6.61 (dd, 2H), 6.06-6.14 (m, 7H), 3.56 (s, 2H, -CH₂-CO), 3.31 (q, 8H, 4CH₂), 2.84 (t, 2H), 2.49 (t, 2H), 1.06 (t, 12H, 4CH₃); ¹³CNMR (CDCl₃): 166.18, 165.02, 154.18, 153.72, 149.53, 149.26, 148.99, 136.39, 133.69, 132.96, 131.60, 130.50, 129.32, 128.74, 127.59, 124.1, 123.57, 122.03, 116.90, 109.01, 108.48, 103.98, 98.19, 67.11, 44.80, 41.67, 40.54, 40.13, 13.04; ESI-MS m/z 669.0028 [M+H⁺, 60%], Calc.: 669.347 [M+H⁺].



Scheme 1 Synthesis of L^1

Synthesis of L-Al complex as [Al(L)(NO₃)₂]

To a 10 mL ethanolic solution of L¹ (0.01mmol), a solution of aluminium nitrate was added dropwise and stirred for 4 h. Solvent was removed using a rotary evaporator, while a blood red solid was obtained (Scheme S1†).

[Al(L)(NO₃)₂]: C₄₁H₄₃AlN₈O₉; Anal. Found: C, 59.89; H, 5.16; N, 13.91; Calc.: C, 60.14; H, 5.29; N, 13.68. IR (cm⁻¹): ν_{NH}, 3437; ν_{C=C}, 2845; ν_{C=O}, 1691; ν_{C=N}, 1612; ¹HNMR (500 MHz, CDCl₃): 11.18 (s, 1-NH-CO), 8.76 (dd, 1H), 8.52 (dd, 1H), 8.11 (dd, 1H), 7.93 (dd, 1H), 7.87 (dd, 1H), 7.46 (dd, 2H), 7.39 (m, 1H), 7.08 (dd, 2H), 6.36 (t, 1H), 6.22 (d, 1H), 6.19 (d, 1H), 6.15 (d, 1H), 3.89 (s, 2H, -CH₂-CO), 3.33 (q, 8H, 4CH₂), 2.94 (t, 2H), 2.59 (t, 2H), 1.09 (t, 12H, 4CH₃); ¹³CNMR (DMSO-d₆): 169.73, 169.10, 154.89, 154.50, 153.49, 150.12, 149.42, 134.44, 134.17, 130.23, 129.42, 129.11, 128.91, 127.88, 124.46, 124.15, 123.53, 123.23, 117.10, 109.15, 104.88, 104.68, 98.12, 47.02, 44.58, 38.64, 38.19, 13.20; ESI-MS in methanol: [M + CH₃OH + H]⁺, m/z, 851.4242 (obsd. with 11 % abundance) (Calc.: m/z, 851.85; where M = [Al(L)(NO₃)₂]).

General method of UV-vis and fluorescence titration

Path length of the cells used for absorption and emission studies was 1 cm. For UV-vis and fluorescence titrations, stock solution of L¹ was prepared in HEPES buffer (1 mM, pH 7.4; 2% EtOH) at r.t. Working solutions of L¹ and Al³⁺ ions were prepared from their respective stock solutions. Fluorescence measurements were performed using 5 nm x 5 nm slit width. All the fluorescence and absorbance spectra were taken after 30 minutes of mixing of Al³⁺ ions and L¹ to acquire the optimised spectra.

A series of solutions containing L¹ and Al(NO₃)₃ were prepared such that the total concentration of L¹ (10 μM) remain constant in all the sets. The mole fraction (X) of Al³⁺ ions was varied from 0.1 to 0.6. The absorbance at 561 nm was plotted against the mole fraction of the probe for stoichiometry determination.

Emission study

Organic moiety (L¹) shows a very weak emission at 588 nm in HEPES buffer (1 mM, pH 7.4; 2% EtOH) at 25 °C when excited at 550 nm considering the absorption at 561 nm. Fluorescence quantum yields (Φ) were estimated by integrating the area under the fluorescence curves with the equation:

$$\Phi_{\text{sample}} = \Phi_{\text{ref}} X \frac{\text{OD}_{\text{ref}} \times A_{\text{sample}} \times \square_{\text{sample}}^2}{\text{OD}_{\text{sample}} \times A_{\text{ref}} \times \square_{\text{ref}}^2}$$

where A is the area under the fluorescence spectral curve and OD is optical density of the compound at the excitation wavelength, 550 nm, □ is the refractive index of the solvent used. The standard used for the measurement of fluorescence quantum yield was rhodamine-B (Φ = 0.7 in ethanol).

Calculation of Förster distance (R₀)

The Förster distance (R₀) for the FRET process was calculated from the following simplified equation below:^{21,22}

$$R_0 = 0.211 [k^2 \eta^{-4} \Phi_D J_{DA}]^{1/6} \\ = 0.211 [k^2 \eta^{-4} \Phi_D \int_0^\infty I_D(\lambda) \epsilon_A(\lambda) \lambda^4 d\lambda]^{1/6} \text{ (in \AA)}$$

where η is the refractive index (η = 1.33 in water),²³ Φ_D is the

quantum yield of the donor; k denotes the average squared orientational part of a dipole-dipole interaction, typically k² = 2/3;²⁴ J_{DA} expresses the degree of spectral overlap between the donor emission and the acceptor absorption; I_D(λ) is the normalized fluorescence spectra of the donor; ε_A(λ) is the molar absorption coefficient of the acceptor.

Preparation of cell and *in vitro* cellular imaging with L¹

Human cervical cancer cell, HeLa cell line was purchased from National Center for Cell Science (NCCS), Pune, India and was used throughout the study. Cells were cultured in Dulbecco's modified Eagle's medium (DMEM, Gibco BRL) supplemented with 10% FBS (Gibco BRL), and 1% antibiotic mixture containing penicillin, streptomycin and neomycin (PSN, Gibco BRL), at 37 °C in a humidified incubator with 5% CO₂. For experimental study, cells were grown to 80-90 % confluence, harvested with 0.025 % trypsin (Gibco BRL) and 0.52 mM EDTA (Gibco BRL) in PBS (phosphate-buffered saline, Sigma Diagnostics) and plated at desire cell concentration and allowed to re-equilibrate for 24 h before any treatment. Cells were rinsed with PBS and incubated with DMEM-containing L¹ (10 μM, 1% DMSO) for 30 min at 37 °C. All experiments were conducted in DMEM containing 10% FBS and 1% PSN antibiotic. The imaging system was composed of a fluorescence microscope (ZEISS Axioskop 2 plus) with an objective lens [10×].

Cell cytotoxicity assay

To test the cytotoxicity of L¹, MTT [3-(4,5-dimethyl-thiazol-2-yl)-2,5-diphenyl tetrazolium bromide] assay was performed by the procedure described earlier.²⁵ After treatments of the probe (5, 10, 20, 50, and 100 μM), 10μl of MTT solution (10 mg/mL PBS) was added in each well of a 96-well culture plate and incubated continuously at 37 °C for 6 h. All mediums were removed from wells and replaced with 100μl of acidic isopropanol. The intracellular formazan crystals (blue-violet) formed were solubilized with 0.04 N acidic isopropanol and the absorbance of the solution was measured at 595 nm wavelength with a microplate reader. Values are means ± S.D. of three independent experiments. The cell cytotoxicity was calculated as percent cell cytotoxicity = 100% cell viability.

Result and discussion

Synthesis and characterisation

The rhodamine B-en carboxamide (1) was obtained by converting rhodamine B following a literature method,¹⁹ and 2-chloro-N-(quinolin-8-yl)acetamide (2) was prepared from the reaction of 2-chloroacetyl chloride and 8-aminoquinoline in chloroform medium in presence of NEt₃ (Scheme 1). After that, the probe, L¹ was isolated from the reaction of rhodamine B-en carboxamide and 2-chloro-N-(quinolin-8-yl)acetamide in a dry acetonitrile solution in presence of anhydrous K₂CO₃. The formulation of L¹ was confirmed by physico-chemico and spectroscopic methods (Fig. S1A-D†). The L-Al complex was obtained when aluminium nitrate was mixed with the ethanolic solution of L¹ under stirring condition. After removing the solvent a blood red colored solid was obtained (Scheme S1†). The formulation of L-Al complex was confirmed by physico-chemico and spectroscopic tools (Fig. S2A-D†).

UV-vis spectroscopic studies of L^1

UV-vis spectra of L^1 was recorded in HEPES buffer (1 mM, pH 7.4; 2% EtOH) at 25 °C shows an absorption maximum at 318 nm which may possibly be attributed to the intramolecular π - π^* charge transfer (CT) transition. On stepwise addition of Al^{3+} ions (0-30 μ M) to the solution of L^1 in HEPES buffer (1 mM, pH 7.4; 2% EtOH), the absorption intensity at 318 nm was increased gradually and a new peak at 561 nm (Fig. 1) was generated due to the formation of pink color from the colorless solution (Fig. 2). Considering the complexity of the intracellular environment, an additional experiment of the probe was performed to determine whether the other ions were potential interferents or not. To establish this fact, metal ion selectivity assays were performed while keeping the other experimental condition unchanged. No significant change in the UV-vis spectral pattern was observed upon the addition of 10 equivalents excess of relevant metal ions *i.e.* Na^+ , K^+ , Ca^{2+} , Mg^{2+} , Cr^{3+} , Mn^{2+} , Fe^{3+} , Co^{2+} , Ni^{2+} , Zn^{2+} , Cd^{2+} , Hg^{2+} , Cu^{2+} and Pb^{2+} .

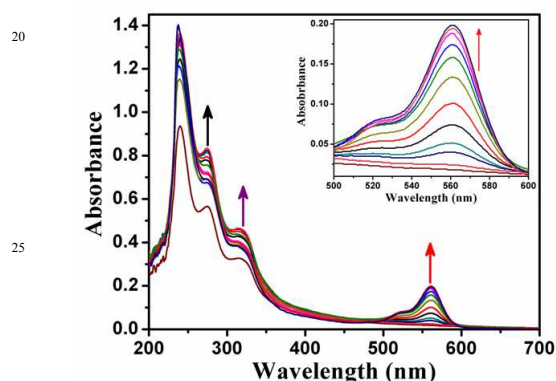


Fig. 1 UV-vis titration spectra of L^1 (10 μ M) upon incremental addition of Al^{3+} ions (0-30 μ M) in HEPES buffer (1 mM, pH 7.4; 2% EtOH)



Fig. 2 Naked eye visual and fluorescence color change (A) probe, L^1 only, (B) in presence of Al^{3+} ions in HEPES buffer (1 mM, pH 7.4; 2% EtOH)

The complex formed between L^1 and Al^{3+} was found to be 1:1 in stoichiometry, which has been established with the help of Job's plot (Fig. S3†) using the absorbance data. Further confirmation of 1:1 stoichiometry with probable formulation of L-Al complex was established by the physico-chemical and spectroscopic data of the L-Al complex isolated in the solid form. The molecular-ion peak in ESI-MS of L- Al^{3+} was observed at m/z 851.4242 evidenced to the 1:1 stoichiometric species (Fig. S2B†).

Fluorescence spectroscopic studies of L^1

To optimize the pH of the experimental condition, a pH study has been performed to control the efficiency of the probe (L^1). In absence of Al^{3+} ions, L^1 exhibited fluorescence of weak intensity and showed an interesting pH independency over the pH range 6.0 to 10.0 (Fig. S4†). At low pH the probe showed high emission intensity due to the fact that at low pH the spirolactam ring opens irrespective of metal ions added.^{18a,26} It was also noticed that the presence of Al^{3+} ions enhances the emission intensity of L^1 significantly at pH 4.0-10.0. The emission spectrum of the L^1 excited at 350 nm exhibits a fluorescence maximum at 470 nm in HEPES buffer (1 mM, pH 7.4; 2% EtOH) at 25 °C. The intensities at 470 nm were significantly decreased with a concomitant increase in intensities at 588 nm through an isoemissive point at *ca.* 553 nm, when various concentrations of Al^{3+} ions (0-30 μ M) were added (Fig. 3).

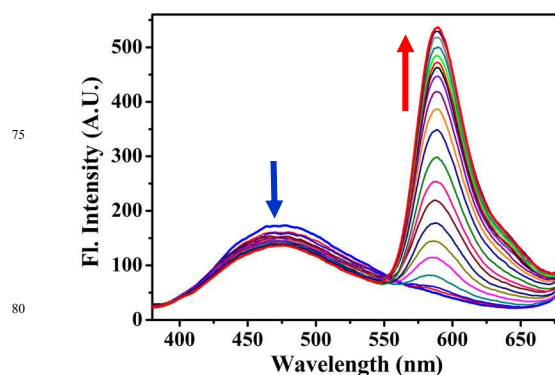


Fig. 3 Emission spectra of L^1 (10 μ M) in presence of Al^{3+} ions (0-30 μ M) at λ_{ex} = 350 nm in HEPES buffer (1 mM, pH 7.4; 2% EtOH) at 25 °C

Ratiometric signaling of fluorescence output at two different wavelengths plotted as a function of concentration of Al^{3+} ions indicates that the fluorescence intensity ratio of wavelength 470 nm and 588 nm (I_{588}/I_{470}) gradually increases with increase of the concentration of Al^{3+} ions (Fig. 4). L^1 exhibited a near about 75-fold increase of its fluorescence intensity upon addition of only 3.0 equivalent of Al^{3+} ions.

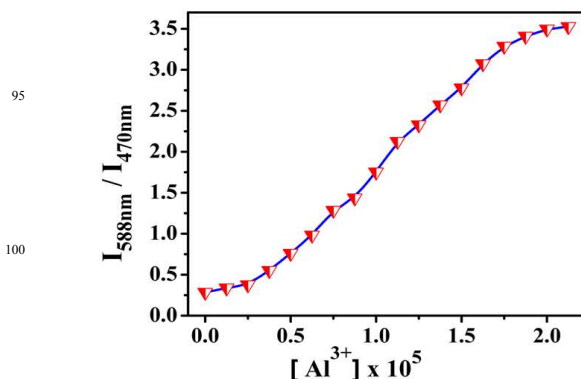


Fig. 4 Ratiometric signaling of fluorescence output at two different wavelengths is plotted as a function of concentration of Al^{3+} ions in aq. HEPES buffer

From the plot of the fluorescence intensity at 588 nm (I_{588}) versus $[Al^{3+}]$ it is reflected that L^1 could be used to detect Al^{3+} ions as low as *ca.* 33 nM (Fig. S5†).²⁷ To calculate the detection

limit the calibration curve (Fig. S6†) in the lower region were obtained. From the slope of the curve (S) and the standard deviation of seven replicate measurements of the zero level (σ_{zero}) the detection limit was estimated using the equation $3\sigma/S$.^{17,28}

This study indicates that the detection limit of **L**¹ for Al³⁺ ions was found to be 6.19×10^{-9} M, which is comparable to the previously reported FRET-based Al³⁺ ion selective fluorescent sensor^{16b} but it is superior to that report as here the FRET process is taking place in aqueous solution.

A metal ion selectivity study was then performed for **L**¹ to understand this phenomenon under identical experimental conditions. Interestingly, the introduction of other metal ions causes the fluorescence intensity to be either unchanged or weakened. Fluorescence enhancement of **L**¹ (10 μ M) was not observed upon addition of excess 50 equivalents of biologically relevant metal ions *i.e.* Na⁺, K⁺, Ca²⁺, Mg²⁺ and 10 equivalents excess of several competitive metal ions [Cr³⁺, Mn²⁺, Fe³⁺, Co²⁺, Ni²⁺, Zn²⁺, Cd²⁺, Hg²⁺, Cu²⁺ and Pb²⁺] (Fig. S7†), and also no color change found in visual naked eye detection (Fig. S8 and S9†). In presence of 10 times excess of various tested ions together with **L**¹ and Al³⁺ ions, almost no adverse effect on intensity was observed (Fig. S10†).

As the receptor **L**¹ bears two different fluorophore units, we consider it to be appropriate to study the metal binding event of **L**¹ at two different excitation wavelengths corresponding to the excitation wavelength of the xanthene unit (550 nm) and quinoline unit (350 nm). Fig. 5 showed that excitation of **L**¹ at 550 nm in absence of Al³⁺ did not show any significant emission over the range from 550 to 700 nm initially with a quantum yield of only 0.03. This supports the facts that the receptor remains in the spiroactam form in absence of metal ions, and the nonexistence of the highly conjugated xanthenes form results in the suppression of emission in the above mentioned region. But the addition of Al³⁺ ions to this chemosensor (**L**¹) induces a significant switch ON fluorescence response near 588 nm, showing a visual display of reddish fluorescence with a quantum yield of 0.61 (~20 fold).

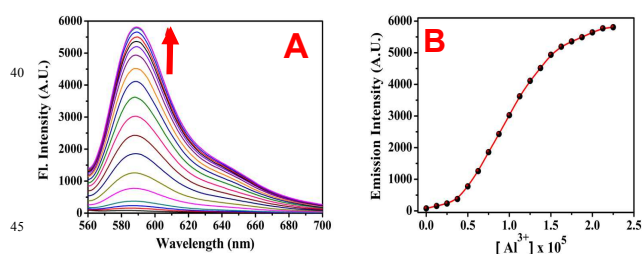
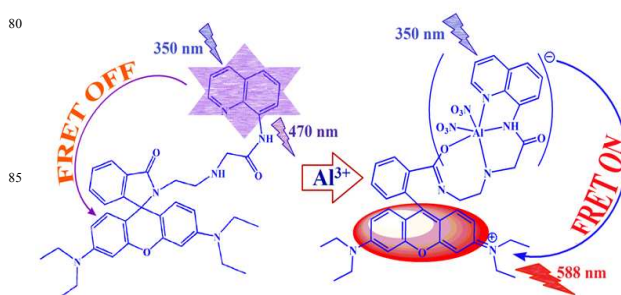


Fig.5 (A) Fluorimetric titration spectra of **L**¹ with Al³⁺ ions (0-30 μ M) at $\lambda_{\text{ex}} = 550$ nm in HEPES buffer (1 mM, pH 7.4; 2% EtOH) at 25 °C, (B) Fluorescence intensity as a function of Al³⁺ ions concentration at $\lambda_{\text{ex}} = 550$ nm in HEPES buffer (1 mM, pH 7.4; 2% EtOH) at 25 °C

Switch ON response for the absorption spectral band at 561 nm and the emission band at 588 nm on binding to Al³⁺ ions suggests the opening of the spiroactam ring of **L**¹ on metal ion coordination (Scheme 2). It is observed that Al³⁺ ion binds with **L**¹ to induce ring-opening of **L**¹ and the generation of xanthene moiety that is selective toward Al³⁺ ions and does not reveal any noticeable spectral change for other tested metal ions together.

The binding of Al³⁺ ions induces opening of the spiroactam

ring of **L**¹ with an associated switch on UV-vis spectral response in the range 380-650 nm, which has a significant spectral overlap with the emission spectrum of the *N*-(quinol-8-yl)-acetamide fragment (Fig. S11†) and this fact unlocks a plausible route for nonradiative transfer of excitation energy from donor quinoline to acceptor xanthene moiety within Förster critical distance (R_0) which was calculated to be 20.03 Å, and initiates an intramolecular FRET process (*viz.* Scheme 2). In the free state of **L**¹ the FRET pathway is totally suppressed, and only an emission maximum near 470 nm was observed when excited at 350 nm. Binding of the receptor to Al³⁺ ions induces the FRET process to produce an intense rhodamine-based reddish emission; *i.e.*, energy transfer from *N*-(quinol-8-yl)-acetamide moiety to xanthene is due to the ring-opening²⁹ resulting in increase of overlap integral between *N*-(quinol-8-yl)-acetamide and xanthene moiety. Thus, when titrated with Al³⁺ ions the emission band at *ca.* 470 nm starts to decrease along with a concomitant generation of a new fluorescence band at *ca.* 588 nm. This change in fluorescence was clearly visualised and the fluorescence color is significantly red (*viz.* Fig. 2).



Scheme 2 Probable mechanism of Al³⁺ ions induced FRET process

The apparent binding constant (K) was determined using the modified Benesi-Hilderbrand method³⁰ and it was found to be 5.81×10^6 M⁻¹ (Fig. S12†). The ring-opening phenomenon is also supported by the ¹³C NMR analyses of **L**¹ and L-Al complex. In the ¹³C NMR spectrum of **L**¹, the signal at $\delta = 67.114$ ppm assignable for the tertiary carbon (sp³-hybridized) of the spiroactam ring in **L**¹ (C₆) is absent in the spectrum of L-Al complex, but appear at $\delta = 134.44$ ppm due to the conversion of C₆ from sp³ to sp²-hybridized carbon, and this feature supports the opening of the spiroactam ring (Fig. 6).³¹

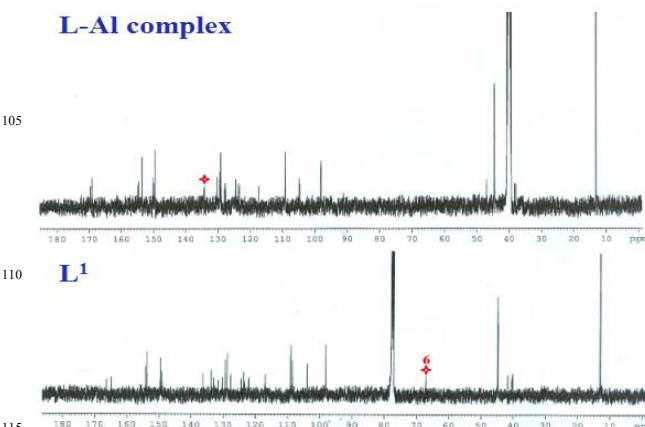


Fig. 6 ¹³C NMR spectra of **L**¹ in CDCl₃ and L-Al complex in dms_o-d₆

In ^1H NMR titration shifting of the corresponding characteristic peaks into the downfield was observed in support of the chelation of L^1 in solution state (Fig. S13 \dagger). The peaks at $\delta = 3.56$ ppm assignable for $-\text{CH}_2-\text{CO}$ protons and $\delta = 10.91$ ppm for NH-CO proton appeared in the spectrum of L^1 (*viz.* Fig. S1C) are significantly shifted to $\delta = 3.89$ ppm and 11.18 ppm respectively (*viz.* Fig. S2C).

The occurrences of FRET process also resemble with the fluorescence lifetime data (Fig. 7, Tables 1). In the fluorescence life time experiment ($\lambda_{\text{em}} = 470$ nm), the average lifetime of L^1 was found to be 12.87 ns. After addition of Al^{3+} ions to the solution of L^1 , the average lifetime ($\lambda_{\text{em}} = 470$ nm) of the complex species decreased to 11.15 ns to 8.37 ns respectively when the concentration of Al^{3+} ions enhanced from 0.5 equivalent to 1.0 equivalent w.r.t. L^1 . On the contrary, the average lifetime of the probe, L^1 increased from 1.60 ns to 9.77 ns ($\lambda_{\text{em}} = 588$ nm) when Al^{3+} ions was added to the solution of L^1 , which resembles the Al^{3+} ions induced FRET process (Fig. S14 \dagger).

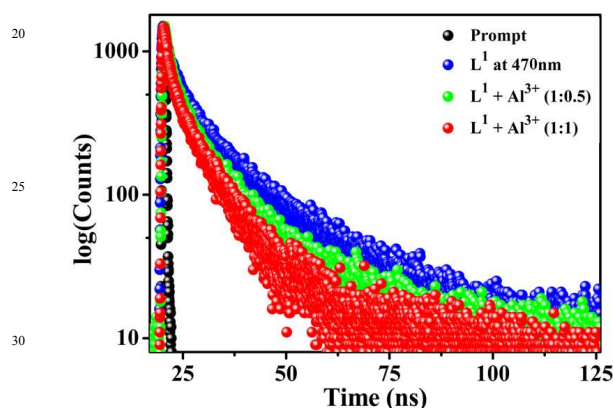


Fig. 7 Time resolved fluorescence decay of L^1 ($10\mu\text{M}$) only and in presence of added Al^{3+} ions in HEPES buffer (1 mM, pH 7.4; 2% EtOH) at 25°C using a nano LED of 377 nm as the light source at $\lambda_{\text{em}} = 470\text{nm}$

Table 1 Fluorescence life time (ns) of the corresponding of L^1 and L-Al complex at $\lambda_{\text{em}} = 470$ nm

$\lambda_{\text{em}} = 470$ nm	τ_{av} (ns)	χ^2	ϕ	$k_r(10^8\text{s}^{-1})$	$k_{\text{nr}}(10^9\text{s}^{-1})$
L^1	12.87	1.1	0.26	0.2020	0.0575
$\text{L}^1 + \text{Al}^{3+}(1:0.5)$	11.15	1.2	-	-	-
$\text{L}^1 + \text{Al}^{3+}(1:1)$	8.37	1.05	0.14	0.1673	0.1028

According to the equations: $^3\tau^{-1} = k_r + k_{\text{nr}}$ and $k_r = \Phi/\tau$, where k_r = the radiative rate constant, and k_{nr} = total nonradiative rate constant, the values of k_r and k_{nr} for the organic moiety, L^1 and L-Al species were listed in Table 1 and 2. The data in Table 2 suggest that k_r has just slightly changed but the factor that induces fluorescent enhancement is mainly ascribed to the decrease of k_{nr} .

Table 2 Fluorescence life time (ns) of the corresponding of L^1 and L-Al complex at $\lambda_{\text{em}} = 588$ nm

$\lambda_{\text{em}} = 588$ nm	τ_{av} (ns)	χ^2	ϕ	$k_r(10^8\text{s}^{-1})$	$k_{\text{nr}}(10^9\text{s}^{-1})$
L^1	1.6013	1.1	0.03	0.1873	0.60576
$\text{L}^1 + \text{Al}^{3+}(1:0.5)$	2.065	1.00	-	-	-
$\text{L}^1 + \text{Al}^{3+}(1:1)$	9.7729	1.05	0.61	0.6242	0.03990

Biological studies of L^1 in presence of Al^{3+}

To examine the utility of the probe in biological systems, it was applied to human cervical cancer HeLa cell. In these experiments both the Al^{3+} ions and L^1 was allowed to uptake by the cells of interest and the images of the cells were recorded by the fluorescence microscopy following excitation at ~ 550 nm. After incubation with L^1 ($10\mu\text{M}$) for 30 min, the cells displayed very faint intracellular fluorescence. However, cells exhibited intensive fluorescence when exogenous Al^{3+} ions were introduced into the cell *via* incubation with Al-salt (Fig. 8). The fluorescence responses of the probe with various concentrations of added Al^{3+} ions are clearly evident from the cellular imaging. In addition, the *in vitro* study showed that $10\mu\text{M}$ of L^1 did not show no cytotoxic effect to cell upto 6 h (Fig. S15 \dagger). These results indicate that the probe has a huge potentiality for both *in vitro* and *in vivo* application as Al^{3+} ions sensor.

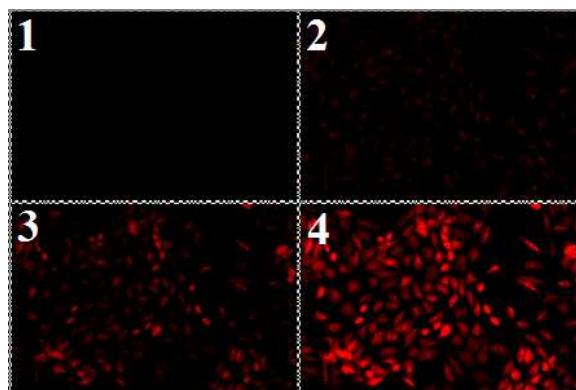


Fig. 8 Fluorescence image of HeLa cells after incubation with L^1 for 30 min followed by treatment with (1) $0\mu\text{M}$; (2) $3\mu\text{M}$; (3) $5\mu\text{M}$; (4) $10\mu\text{M}$ Al^{3+} ions at 37°C respectively and the samples were excited at ~ 550 nm.

Conclusions

In summary, we may conclude that a newly designed fluorescent chemosensor (L^1) behaves as a highly specific and selective FRET-based ratiometric fluorescence probe towards Al^{3+} ions that can also be detected by naked eye due to the ring-opening of the spirolactam system of rhodamine. The detection limit of this probe, L^1 is very significantly low (6.19×10^{-9} M) comparable with the previously reported FRET-based Al^{3+} ion selective fluorescent sensor and in this regard it may be considered as a superior FRET-based chemosensor for Al^{3+} ions in aqueous solution, so far. This probe may be employed as biomarker for the imaging of the Al^{3+} ions in the living cells.

Acknowledgments

Financial assistance from CSIR, New Delhi, India is gratefully acknowledged. B. Sen wishes to thank to UGC, New Delhi, India for offering him the fellowship. We sincerely acknowledge Prof. Samita Basu and Mr. Ajay Das, Chemical Science Division, SINP, Kolkata for enabling TCSPC instrument and also thankful to Mr. Samya Banerjee, IISc, Bangalore and Dr. B. Mukherjee, IISER, Kolkata for recording the ^1H NMR, ^{13}C NMR and ESI-MS spectra.

Notes and references

^a Department of Chemistry, The University of Burdwan, Golapbag, Burdwan 713104, India. E-mail: pabitracc@yahoo.com

^b Molecular Biology and Genetics Laboratory, Department of Zoology, Kalyani University, India

† Electronic Supplementary Information (ESI) available: [Schemes, characterization data, tables, figures, and some spectra], See DOI: 10.1039/b000000x/

‡ Footnotes should appear here.

Corresponding Author

* E-mail: pabitracc@yahoo.com. Tel: +91-342-2558554 extn. 424. Fax: +91-342-2530452.

- M.G. Sont, S.M. White, W.G. Flamm, G.A. Burdock, *Regul. Toxicol. Pharm.*, 2001, **33**, 66.
- N.W. Bavior, W. Egan, P. Richman, *Vaccine*, 2002, **20**, S18-S23.
- D.P. Perl and A.R. Brody, *Science*, 1980, **208**, 297.
- D.P. Perl, D.C. Gajdusek, R.M. Garruto, R.T. Yanagihara and C.J. Gibbs, *Science*, 1982, **217**, 1053.
- E.H. Jeffery, K. Abreo, E. Burgess, J. Cannata, J.L. Greger, *J. Toxicol. Env. Health*, 1996, **48**, 649.
- A. Becaria, A. Campbell, S.C. Bondy, *Toxicol. Ind. Health*, 2002, **18**, 309.
- J.J. Spinelli, P.A. Demers, N.D. Le, M.D. Friesen, M.F. Lorenzi, R. Fang, R.P. Gallagher, *Cancer Cause Control*, 2006, **17**, 939.
- B. Armstrong, C. Tremblay, D. Baris, G. Theriault, *Am. J. Epidemiol.*, 1994, **139**, 250.
- E. Álvarez, M.L. F-Marcos, C. Monterroso, M.J. F-Sanjurjo, Application of aluminium toxicity indices to soils under various forest species, *For Ecol Manag*, 2005, **211**, 227.
- J. Barceló, C. Poschenrieder, Fast root growth responses, root exudates, and internal detoxification as clues to the mechanisms of aluminium toxicity and resistance: a review, *Environ Exp Bot*, 2002, **48**, 75.
- (a) H. Lian, Y. Kang, S. Bi, Y. Arkin, D. Shao, D. Li, Y. Chen, L. Dai, N. Gan and L. Tian, *Talanta*, 2004, **62**, 43; (b) H. Seol, S.C. Shin, Y.B. Shim, *Electroanal.*, 2004, **16**, 2051; (c) O.Y. Nadzhafova, S.V. Lagodzinskaya, V.V. Sukhan, *J. Anal. Chem.*, 2001, **56**, 178; (d) A.J. Downard, B.O'Sullivan and K.J. Powell, *Anal. Chim. Acta*, 1997, **345**, 5; (e) M.J. Ahmed, J. Hossan, *Talanta*, 1995, **42**, 1135.
- J. R. Lakowicz, Topics in Fluorescence Spectroscopy, in Probe Design and Chemical Sensing, Kluwer Academic Publishers, New York, 2002, vol. 4.
- (a) A.P. de Silva, D.B. Fox, J.M. Huxley and T.S. Moody, *Coord. Chem. Rev.*, 2000, **205**, 41; (b) B. Valeur and I. Leray, *Coord. Chem. Rev.*, 2000, **205**, 3.
- (a) S. Sen, T. Mukherjee, B. Chattopadhyay, A. Moirangthem, A. Basu, J. Marek and P. Chattopadhyay, *Analyst*, 2012, **137**, 3975; (b) S. Sen, T. Mukherjee, S. Sarkar, S. K. Mukhopadhyay and P. Chattopadhyay, *Analyst*, 2011, **136**, 4839; (c) U. C. Saha, K. Dhara, B. Chattopadhyay, S. K. Mandal, S. Mondal, S. Sen, M. Mukherjee, S. V. Smaalen and P. Chattopadhyay, *Org. Lett.*, 2011, **13**, 4510; (d) U. C. Saha, B. Chattopadhyay, K. Dhara, S. K. Mandal, S. Sarkar, A. R. Khuda-Bukhsh, M. Mukherjee, M. Helliwell and P. Chattopadhyay, *Inorg. Chem.*, 2011, **50**, 1213; (e) K. Dhara, U. C. Saha, A. Dan, M. Manassero, S. Sarkar and P. Chattopadhyay, *Chem. Commun.*, 2010, **46**, 1754; (f) M. Mukherjee, B. Sen, S. Pal, M. S. Hundal, S.K. Mandal, A.R. Khuda-Bukhsh and P. Chattopadhyay, *RSC Advances*, 2013, **3**, 19978.
- (a) Neeraj, A. Kumar, V. Kumar, R. Prajapati, S.K. Asthana, K.K. Upadhyay and J. Zhao, *Dalton Trans.*, 2014, **43**, 583 and references therein; (b) S.B. Maity and P.K. Bharadwaj, *Inorg. Chem.*, 2013, **52**, 1161; (c) B.K. Datta, C. Kar, A. Basu and G. Das, *Tetrahedron Lett.*, 2013, **54**, 771; (d) S. Goswami, A. Manna, S. Paul, K. Aich, A.K. Das and S. Chakraborty, *Dalton Trans.*, 2013, **42**, 8078. (e) D. Maity and T. Govindaraju, *Chem. Commun.*, 2012, **48**, 1039; (f) S. Kim, J.Y. Noh, K.Y. Kim, J.H. Kim, H.K. Kang, S.-W. Nam, S.H. Kim, S. Park, C. Kim and J. Kim, *Inorg. Chem.*, 2012, **51**, 3597; (g) X. Sun, Y.-W. Wang and Y. Peng, *Org. Lett.*, 2012, **14**, 3420; (h) Y. Lu, S. Huang, Y. Liu, S. He, L. Zhao and X. Zeng, *Org. Lett.*, 2011, **13**, 5274; (i) M. Arduini, F. Felluga, F. Mancin, P. Rossi, P. Tecilla, U. Tonellato and N. Valentinuzzi, *Chem. Commun.*, 2003, 1606.
- (a) A. Sahana, A. Banerjee, S. Lohar, A. Banik, S.K. Mukhopadhyay, D.A. Safin, M.G. Babashkina, M. Bolte, Y. Garcia and D. Das, *Dalton Trans.*, 2013, **42**, 13311; (b) A. Sahana, A. Banerjee, S. Lohar, B. Sarkar, S.K. Mukhopadhyay and D. Das, *Inorg. Chem.*, 2012, **51**, 11220; (c) M. Arduini, F. Felluga, F. Mancin, P. Rossi, P. Tecilla, U. Tonellato and N. Valentinuzzi, *Chem. Commun.*, 2003, 1606.
- S. Pal, B. Sen, M. Mukherjee, K. Dhara, E. Zangrando, S.K. Mandal, A.R. Khuda-Bukhsh and P. Chattopadhyay, *Analyst*, 2014, **139**, 1628.
- (a) B. Sen, M. Mukherjee, S. Pal, K. Dhara, S.K. Mandal, A.R. Khuda-Bukhsh and P. Chattopadhyay, *RSC Adv.*, 2014, **4**, 14919; (b) S. Sen, S. Sarkar, B. Chattopadhyay, A. Moirangthem, A. Basu, K. Dhara and P. Chattopadhyay, *Analyst*, 2012, **137**, 3335; (c) A. P. de Silva, H. Q. N. Gunaratne, T. Gunnlaugsson, A. J. M. Huxley, C. P. McCoy, J.T. Rademacher and T.E. Rice, *Chem. Rev.*, 1997, **97**, 1515; (d) Z. Xu, Y. Xiao, X. Qian, J. Cui and D. Cui, *Org. Lett.*, 2005, **7**, 889;
- J.S. Wu, I.-C. Hwang, K.S. Kim and J.S. Kim, *Org Lett.*, 2007, **9**, 907.
- X. Zhou, P. Li, Z. Shi, X. Tang, C. Chen and W. Liu, *Inorg Chem.*, 2012, **51**, 9226.
- X. Zhang, Y. Xiao and X. Qian, *Angew. Chem. Int. Ed.*, 2008, **47**, 8025.
- J. R. Lakowicz, *Principles of Fluorescence Spectroscopy*, Springer, 2006, 443.
- G.M. Hale and M.R. Query, *Appl. Opt.*, 1973, **12**, 555.
- J.R. Lakowicz, *Principles of Fluorescence Spectroscopy*, Springer, New York, 2006, pp 443.
- J. Ratha, K.A. Majumdar, S.K. Mandal, R. Bera, C. Sarkar, B. Saha, C. Mandal, K.D. Saha and R. Bhadra, *Mol. Cell Biochem.*, 2006, **290**, 113.
- X. Chen, T. Pradhan, F. Wang, J.S. Kim, and J. Yoon, *Chem. Rev.*, 2012, **112**, 1910.
- A. Caballero, R. Martinez, V. Lloveras, I. Ratera, J. V. Gancedo, K. Wurst, A. Tarraga, P. Molina, J. Veciana, *J. Am. Chem. Soc.*, 2005, **127**, 15666.
- A. Hakonen, *Anal. Chem.*, 2009, **81**, 4555.
- (a) X. Chen, T. Pradhan, F. Wang, J.S. Kim and J. Yoon, *Chem. Rev.*, 2012, **112**, 1910; (b) M. Vendrell, D. Zhai, J.C. Er and Y.T. Chang, *Chem. Rev.*, 2012, **112**, 4391; (c) C. Kar, M.D. Adhikari, A. Ramesh and G. Das, *Inorg. Chem.*, 2013, **52**, 743.
- H. A. Benesi and J. H. Hildebrand, *J. Am. Chem. Soc.*, 1949, **71**, 2703.
- T. Mistri, R. Alam, M. Dolai, S.K. Mandal, P. Guha, A.R. Khuda-Bukhsh and M. Ali, *Eur. J. Inorg. Chem.*, 2013, **2013**, 5854.
- N.J. Turro, *Modern Molecular Photochemistry*, Benjamin/ Cummings Publishing Co., Inc. Menlo Park, CA, 1978.